

Mn valence in lanthanum strontium manganite determined by x-ray photoelectron spectroscopy and electron energy loss spectroscopy



Rolls-Royce



CASE WESTERN RESERVE UNIVERSITY EST. 1826

Shao-Ju Shih¹, Reza Sharghi-Moshtaghin¹, Mark R. De Guire¹, Richard Goettler², Zhien Liu², Shung-Ik Lee² and Arthur H. Heuer¹

1) Dept. of Materials Science and Engineering, Case Western Reserve University, Cleveland, OH 44106;
2) Rolls Royce Fuel Cell Systems USA, North Canton, Ohio 44720

Abstract

Lanthanum strontium manganite ($\text{La}_{1-x}\text{Sr}_x\text{MnO}_{3-y}$) (LSM) is widely used as the cathode in solid oxide fuel cells because of its long-term stability and good performance when operated at higher temperatures (850-900°C). The Mn valence plays an important part in the electrical conductivity, phase stability, and reaction kinetics of the cathode. The Mn valence in turn depends on the level of strontium doping, the ratio of (La+Sr) to Mn, and the operating environment of the cell (temperature and atmosphere). Mn valence is thus one of several important parameters for understanding the relationship between cell and operating conditions. Although the defect chemistry of LSM has been well studied, this is the first study that directly compares measurements of Mn valence from two direct, independent techniques: X-ray photoelectron spectroscopy (XPS) and electron energy loss spectroscopy (EELS). Firstly, both techniques were calibrated against MnO , Mn_2O_3 , and MnO_2 . Then XPS was used to determine Mn valence in several annealed LSM pellets. Lastly, EELS was used to measure Mn valences in LSM at the cathode surface and at the cathode-electrolyte interface, with good agreement between the two techniques.

Mn valence on LSM pellet surfaces: X-ray photoelectron spectroscopy (XPS)

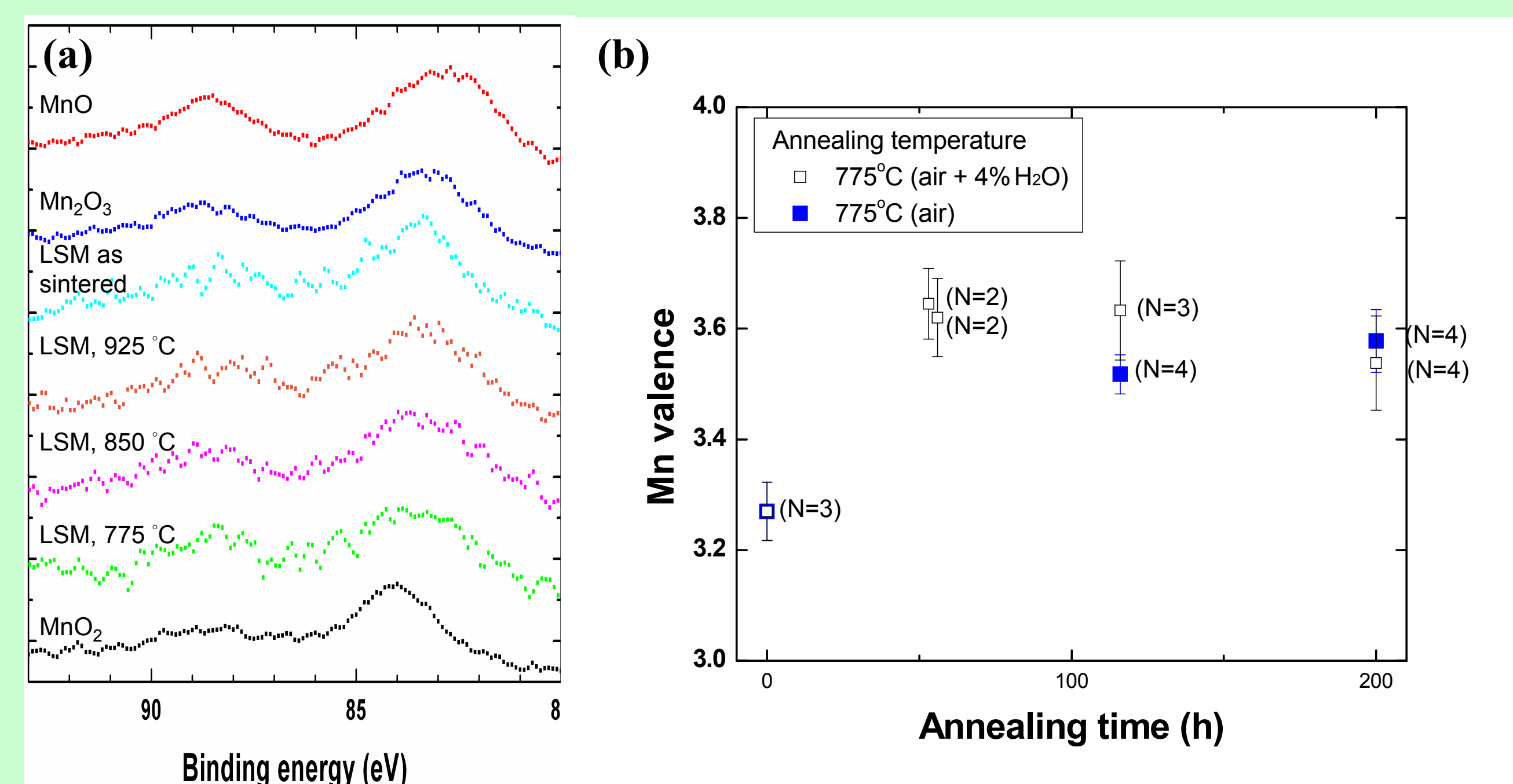


Figure 3. (a) Mn 3s XPS spectra (energy axis referenced to C 1s peak) of reference manganese oxide powders (MnO_2 , Mn_2O_3 and MnO) and LSM pellets annealed for 200 h in air at the indicated temperatures. The splitting of the doublet was used as a measure of the Mn valence in the LSM specimens as a function of (b) time and atmosphere.

Mn valence in LSM near the cathode/electrolyte interface: EELS

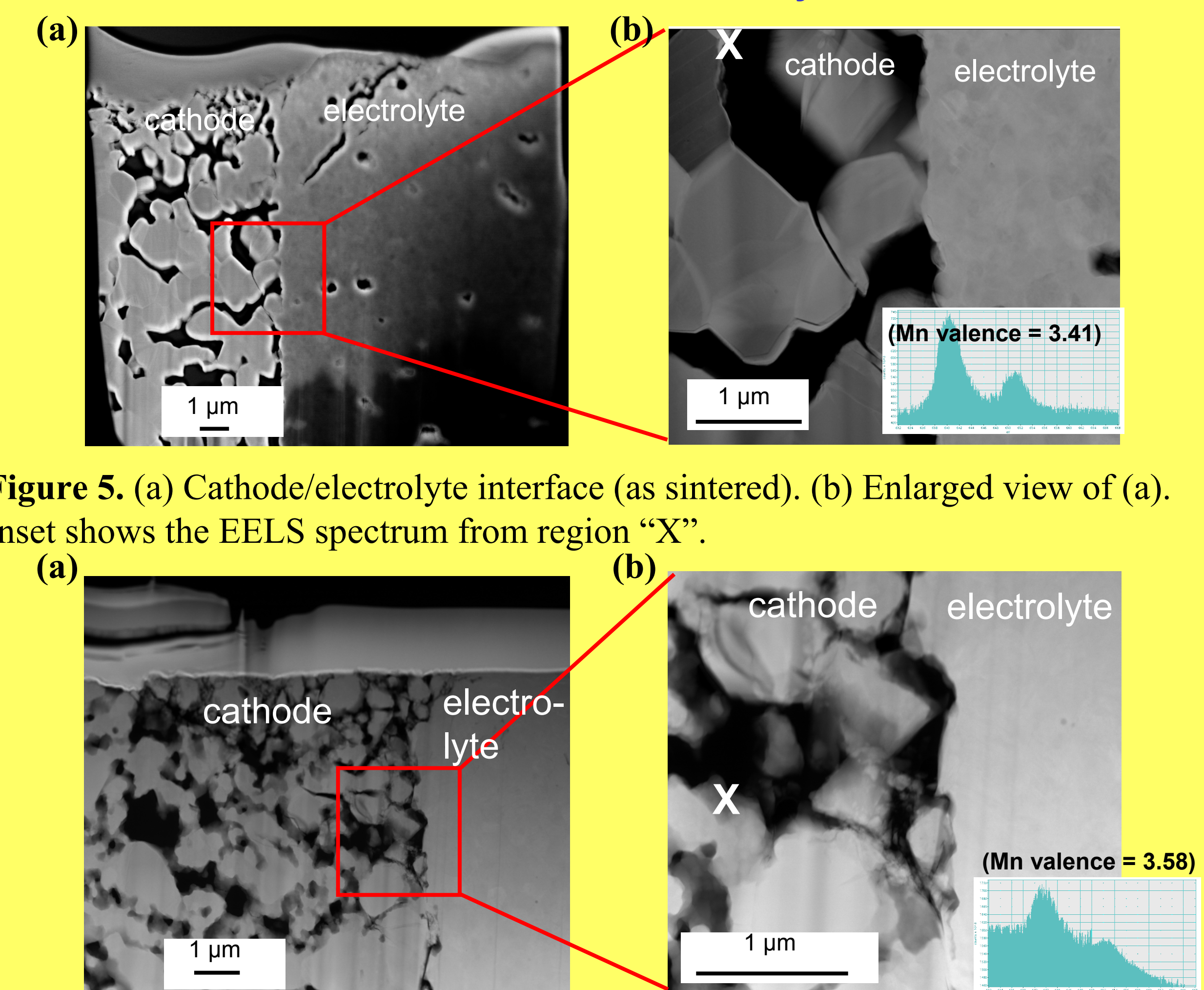


Figure 5. (a) Cathode/electrolyte interface (as sintered). (b) Enlarged view of (a). Inset shows the EELS spectrum from region "X".

Figure 6. (a) Cathode/electrolyte interface of cell operated at 775 ° C for 214 h in air+4% H₂O. (b) Enlarged view of (a). Inset shows the EELS spectrum from region "X".

Area Specific Resistance (ASR) and Mn valence

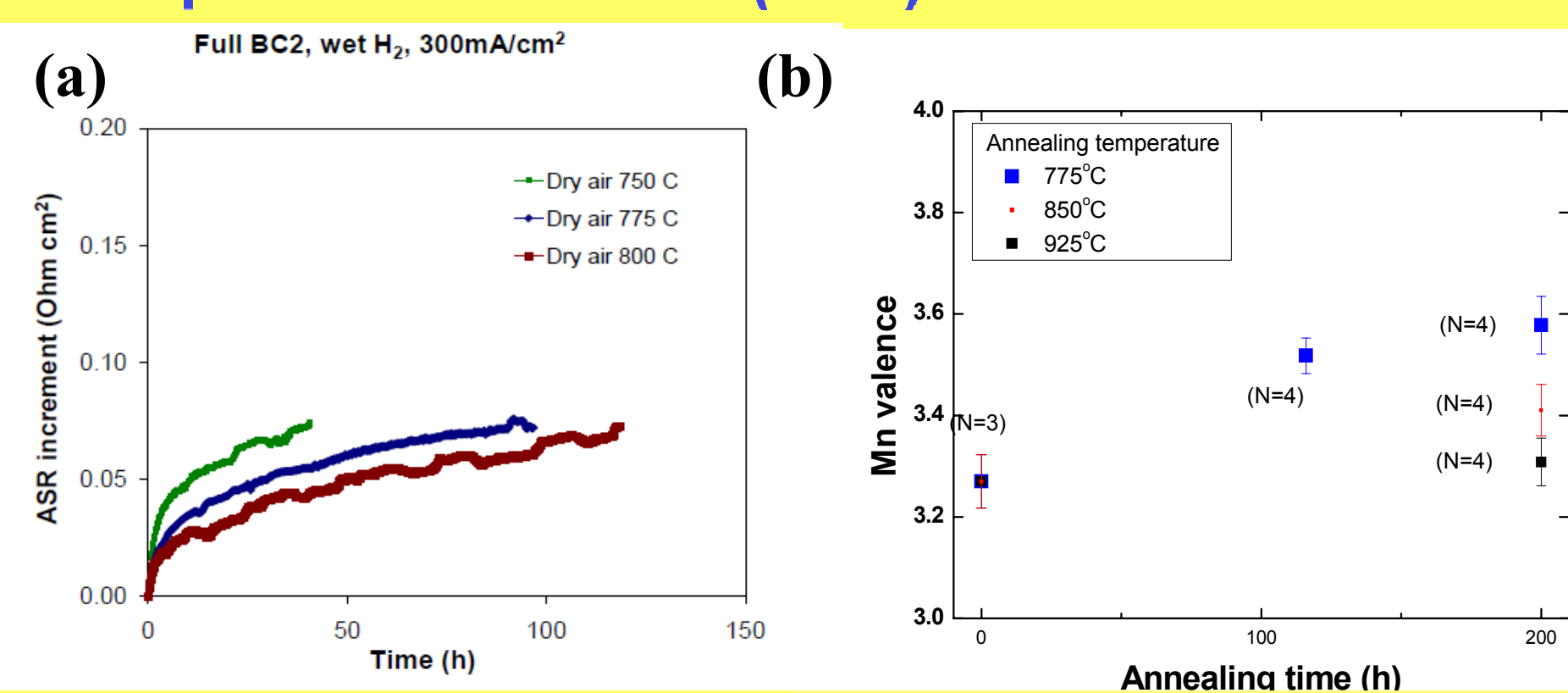


Figure 1. Effect of annealing temperature and time on (a) ASR of button cells and (b) Mn valence in LSM specimen.

X-ray diffraction of lanthanum strontium manganite

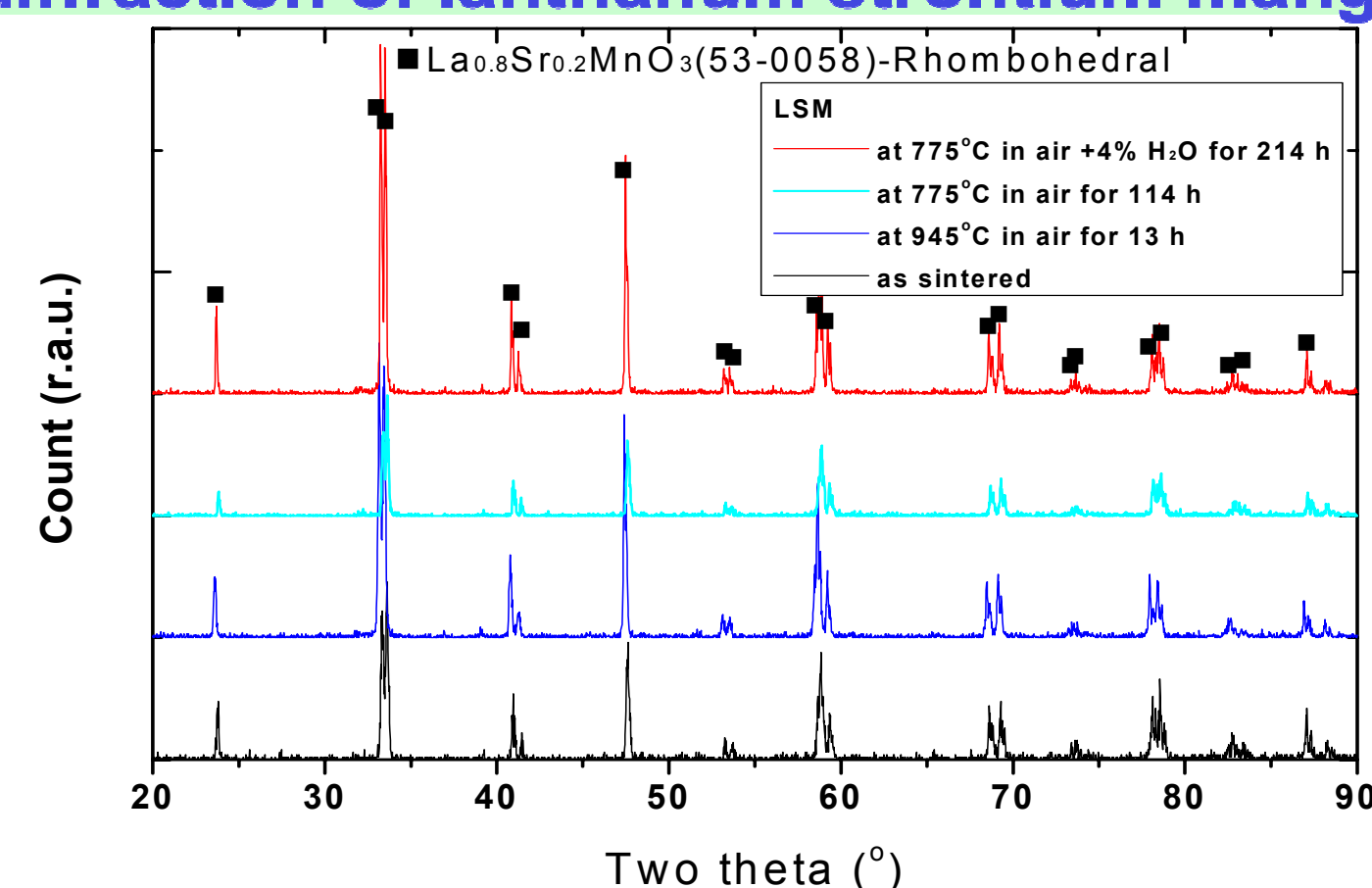


Figure 2. X-ray diffraction patterns of LSM pellets given different annealing conditions.

Comparison of Mn valence determined by XPS & electron energy loss spectroscopy (EELS)

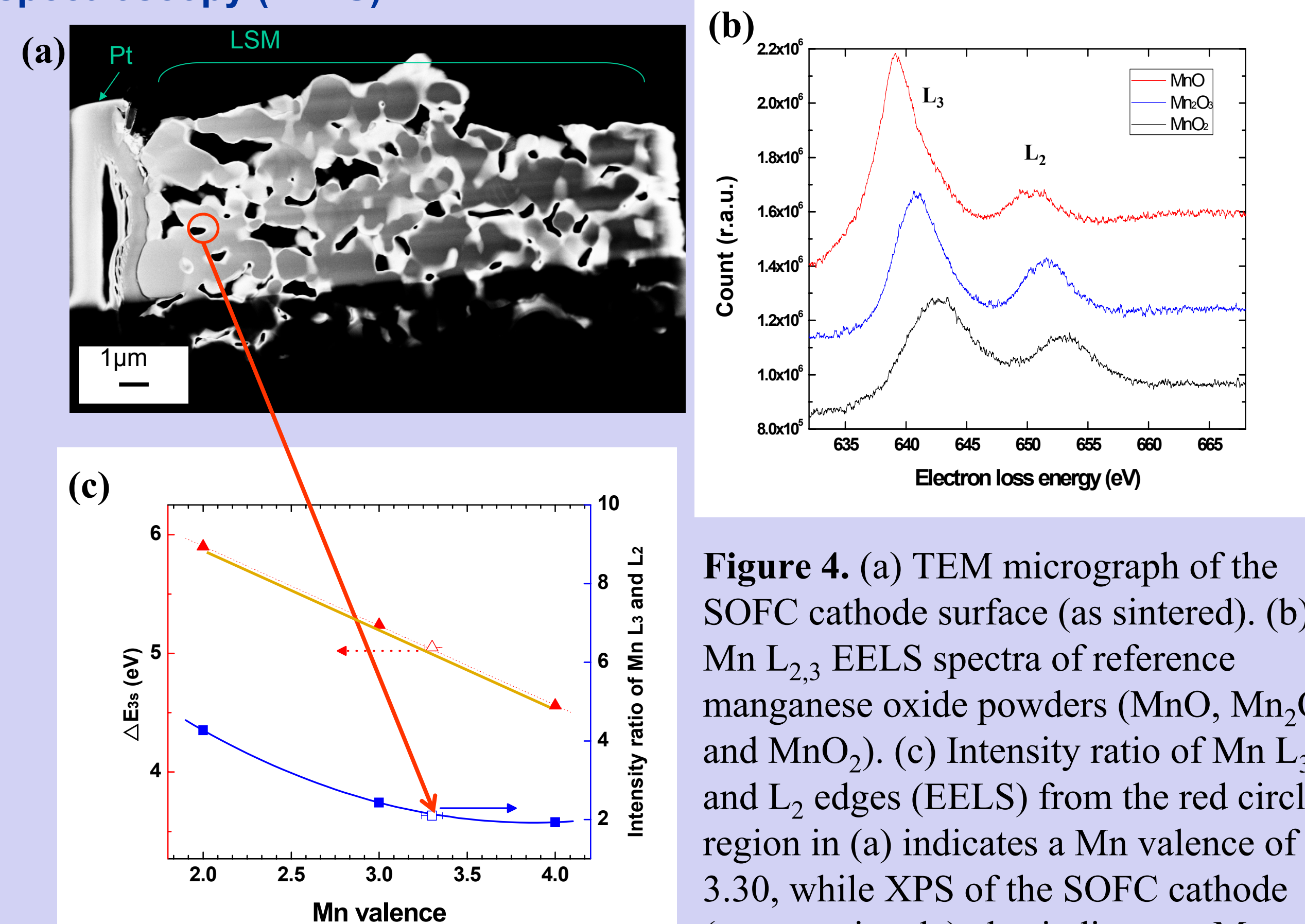


Figure 4. (a) TEM micrograph of the SOFC cathode surface (as sintered). (b) Mn L_{2,3} EELS spectra of reference manganese oxide powders (MnO , Mn_2O_3 and MnO_2). (c) Intensity ratio of Mn L₃ and L₂ edges (EELS) from the red circled region in (a) indicates a Mn valence of 3.30, while XPS of the SOFC cathode (orange triangle) also indicates a Mn valence of 3.30 from the splitting of the Mn 3s peak.

Summary

1. Operation of the SOFC increased the ASR (Fig. 1) more rapidly at 750 °C than at 775 or 800 °C.
2. XRD detected no phase changes in LSM pellets after exposure to air+4% H₂O at 775 °C for 214 h (Fig. 2).
3. XPS showed that annealing LSM pellets in air or air+4% H₂O at 775 °C raised the Mn valence from 3.27 (as sintered) to 3.5-3.6 (Fig. 3).
4. EELS on the as-fired cathode surface shows good agreement in Mn valence with XPS and EELS (3.30 for XPS and 3.30 for EELS) (Fig. 4c).
5. EELS of LSM at the cathode-electrolyte interface showed Mn valences of 3.41 as sintered (Fig. 5) and 3.58 after operation at 775 °C in air+4% H₂O (Fig. 6). These Mn valence changes may be related to the rise in ASR during operation.

References

1. V. R. Galakhov, M. Demeter, S. Bartkowski, M. Neumann, N. A. Ovechkina, E. Z. Kurmaev, N. I. Lobachevskaya, Y. M. Mukovskii, J. Mitchell and D. L. Ederer, *Phys. Rev. B*, **65** (2002) 113102
2. J. L. Mansot, P. Leone, P. Euzen and P. Palradeau, *Microscopy Microanalysis Microstructures*, **5** (1994) 79-90.
3. Z. L. Wang, J. S. Yin and Y. O. Jiang, *Micron*, **31** (2000) 571-580.
4. T. Riedl, T. Gemming and K. Wetzig, *Ultramicroscopy*, **106** (2006) 284-291.

Financial Support

Solid State Energy Conversion Alliance Program, U.S. Department of Energy

